Structural Engineering and Mechanics, *Vol. 83, No. 4 (2022) 415-433*
https://doi.org/10.12989/sem.2022.83.4.415

Experimental shear strengthening of GFRC beams without stirrups using innovative techniques

Marwa Hany*, Mohamed H. Makhlouf[a], Gamal Ismail[b] and Ahmed S. Debaiky[c]

Department of Civil Engineering, Benha Faculty of Engineering, Benha University, Egypt

(*Received October 13, 2021, Revised April 9, 2022, Accepted May 22, 2022*)

Abstract. Eighteen (18) (120×300×2200 mm) beams were prepared and tested to evaluate the shear strength of Glass Fiber Reinforced Concrete (GFRC) beams with no shear reinforcement, and evaluate the effectiveness of various innovative strengthening systems to increase the shear capacity of the GFRC beams. The test variables are the amount of discrete glass fiber (0.0, 0.6, and 1.2% by volume of concrete) and the type of longitudinal reinforcement bars (steel or GFRP), the strengthening systems (externally bonded (EB) sheet, side near-surface mounted (SNSM) bars, or the two together), strengthening material (GFRP or steel) links, different configurations of NSM GFRP bars (side bonded links, full wrapped stirrups, side C-shaped stirrups, and side bent bars), link spacing, link inclination angle, and the number of bent bars. The experimental results showed that adding the discrete glass fiber to the concrete by 0.6%, and 1.2% enhanced the shear strength by 18.5% and 28%, respectively in addition to enhancing the ductility. The results testified the efficiency of different strengthening systems, where it is enhanced the shear capacity by a ratio of 28.4% to 120%, and that is a significant improvement. Providing SNSM bent bars with strips as a new strengthening technique exhibited better shear performance in terms of crack propagation, and improved shear capacity and ductility compared to other strengthening techniques. Based on the experimental shear behavior, an analytical study, which allows the estimation of the shear capacity of the strengthened beams, was proposed, the results of the experimental and analytical study were comparable by a ratio of 0.91 to 1.15.

Keywords: GFRC beam; strengthening technique; (EB) sheet; (SNSM) bars; Steel link; GFRP link

1. Introduction

Shear failure is particularly dangerous since it usually occurs without warning due to steel area reduction due to corrosion, harmful environmental effects, thawing and freezing cycles, physical damage from impacts, and sulfate attack (Noel and Soudki 2011). Fiber Reinforced Concrete (FRC) is widely used in structures, numerous researches studied this subject in the last few decades (Masoud *et al*. 2020, Abdul-Zaher *et al*. 2016, Shoeib *et al*. 2011). FRC has a significant advantage in shear design since it results in reduced shear crack width and the number of cracks. Ata El-kareim *et al*. (2011) examined three R.C. beams with the same distance between stirrups, but with three-volume ratios from discrete glass fiber (0, 0.75, and 1.5 %) to evaluate the shear behavior of discrete glass fiber concrete beams. The experimental investigation resulted that the addition of discrete glass fibers in the concrete mix decreases the formation and extension of cracks, increases durability, increases the residual shear transfer, improves deformation characteristics and sturdiness of concrete.

Concrete beams reinforced and strengthened with fiber-reinforced polymer (FRP) (bars or strips) systems are at the forefront of the rehabilitation of concrete structures, where FRP has a longer service life, is resistant to corrosion, is lightweight, resistant to humidity, has a low thermal expansion, low maintenance, good non-magnetic properties and is proven to increase the shear capacity of RC beams (LiuJin *et al*. 2020, Ayesha *et al*. 2019, Rendy *et al*. 2109, Abdul Saboor *et al*. 2019, Amer *et al*. 2017, Mu'taz Kadhim 2016, Rajai and Mohsen 2016, Chen *et al*. 2012, Chen *et al*. 2010, Bukhari *et al*. 2010). Monika *et al*. (2017) and the authors El-Sayed *et al*. (2005b) used various types and ratios of FRP bars for reinforcing normal concrete beams without stirrups instead of traditional steel and investigated the effect on shear capacity. Several types of research studied the shear strengthening in normal concrete by using variable strengthening techniques of the near-surface mounted (NSM) method and externally bonded reinforcement (EBR) (Minu and Mohsen 2018, Seo *et al*. 2016, Sharaky *et al*. 2015). NSM is a viable alternative to the externally bonded reinforcing (EBR) technique for RC structures Because the application of NSM FRP does not need surface preparation work (Zhanga and Yua 2017, Khalifa 2016), requires less time to install, can avoid harm from external causes such as mechanical damage, fire, and vandalism, enhances the load-carrying capacity of RC elements, produces greater strain in FRP (De Lorenzis 2007), and increases confinement offered by the

*Corresponding author, Ph.D. Student
E-mail: marwa.hani@bhit.bu.edu.eg
[a]Assistant Professor
E-mail: mohamedmakhlouf83@yahoo.com
[b]Professor
E-mail: gamal.ismail@bhit.bu.edu.eg
[c]Professor
E-mail: debaiky@hotmail.com

Copyright © 2022 Techno-Press, Ltd.

ISSN: 1225-4568 (Print), 1598-6217 (Online)

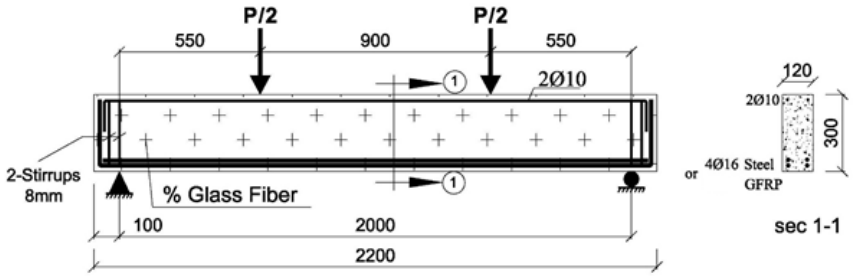

Fig. 1 Longitudinal and cross-section detailing for GFRC beams

surrounding concrete and adhesive, resulting in a lower chance of de-bonding (El-Hacha *et al*. 2004). Dias and Barros (2010, 2012a) applied unidirectional U-shaped CFRP sheets to evaluate the effectiveness of the NSM and EBR CFRP-strengthening procedures. They determined that the NSM approach was more successful than EBR because it produced a greater increase in load-carrying capacity as well as stiffness following shear fracture development, as well as higher values of maximum stresses recorded in the CFRP. The NSM and the EBR shear-strengthened beam presented 90% and 79% of the maximum load of the reference beam, according to Dias and Barros (2012a). This research reports the results from eighteen GFRC beams divided into four groups, the first group investigate the effect of adding glass fiber in concrete mixes with a volume ratio of (0, 0.6, 1.2%) on the shear behavior of RC beams without web reinforcement, the beams in this group were reinforced with steel or GFRP bars as main reinforcement. The other three groups include GFRC beams with a fiber ratio of 1.2% only, reinforced with steel bars as main reinforcement, and strengthened using variable innovative strengthening techniques. The second group is strengthened by GFRP or steel side near-surface mounted (SNSM) links, where bars are vertical or inclined (steel vertical bars had variable spacing). The third group is strengthened by GFRP NSM C- shape stirrups, GFRP NSM full wrap stirrups, or GFRP EBR sheets. The fourth group is strengthened with GFRP side NSM bent bars only as a new innovative strengthening technique in one or two rows, or with combined GFRP SNSM bent bars and GFRP EBR sheets together. The test results showed a higher shear strength, first cracking load, ultimate shear capacity, modulus of elasticity, and maximum deflection by increasing the glass fiber ratio in the concrete mix. The mechanical properties of beams reinforced with steel and GFRP bars were evaluated. Twelve GFRC beams strengthened with innovative techniques were experimentally tested. The cracking load, ultimate shear capacity, and load-deflection curves, deflection, ductility, stiffness, Toughness, strain, and mode of failure were observed and discussed. A shear strength formulation for GFRC beams without web reinforcement was proposed to simulate the experimentally tested beams. Additionally, variable strengthening techniques have been performed to investigate it's effect on shear strength. Whereas Design codes present formulation to calculate the shear strength of reinforced normal concrete beams with web reinforcement, but there is no published formulation to calculate the shear strength of GFRC without web reinforcement, GFRP as main reinforcement, and GFRP bent bars as external shear reinforcement. Finally, the shear strength of glass fiber reinforced concrete beams were assessed by the results of experimental tests.

Research significance

Many researchers used steal FRC to assess the shear behavior of beams, but GFRC beams are used a little in literature. This research aims to study the efficiency of using discrete glass fibers in the concrete mix on the shear behavior of R.C. beams. Moreover, discuss the shear behavior of GFRC beams reinforced with longitudinal steel or GFRP bars that have the same fiber volume ratio. This research study the shear capacity of twelve GFRC beams without stirrups strengthened with innovative different GFRP and steel techniques, which are rarely found in the literature which used fiber concrete. This paper aims to contribute to a better equation of the shear behavior of GFRC beams strengthened externally with different GFRP and steel techniques. The current code formulations do not exist for GFRC beams. The test results allow us to assess the quality of both the existing and proposed design procedures. Finally, the test failure loads $V_{n(\exp)}$ is compared with the prediction shear values of analytical shear force prediction of proposed equations $V_{n(\text{ana})}$.

2. Experimental procedure

2.1 Specimens and test matrix

The experimental program consisted of eighteen beams divided into four groups. All beams had the same concrete dimensions (120×300 mm) and top reinforcement (2bars with 10 mm diameter (2Ø10 steel)) and had no internal stirrups between two supports but had two stirrups out two supported with 40 mm spacing. All specimens except three of these were reinforced by four high tensile steel bars of 16 mm diameter (4Ø16 steel) as main reinforcement, and the remaining three beams (B0GF-F1, B1GF-F1, B2GF-F1) were reinforced by four GFRP bars of 16 mm diameter (4Ø16 GFRP) as main reinforcement. The total span was 2200 mm, while the loaded span was 2000 mm and the respective overhang length of 100 mm. Fig. 1 shows Longitudinal and cross-section detailing for un-strengthened beams in Group No. 1 and base beams for strengthened GFRC beams in Group No. 2, 3, 4. The nomenclature and characteristics of the shear strengthening

Table 1 Experimental program

Group no.	specimen	Fiber Ratio (μ) %	AS Bars	Strengthening systems (S.S)
1	B0GF-S1	0%	4Ø16 steel	……
	B1GF-S1	0.6%	4Ø16 steel	……
	B2GF-S1	1.2%	4Ø16 steel	……
	B0GF-F1	0%	4Ø16 GFRP	……
	B1GF-F1	0.6%	4Ø16 GFRP	……
	B2GF-F1	1.2%	4Ø16 GFRP	……
2	B2GF-V20S	1.2%	4Ø16 steel	Steel links, S20,90°, two sides, NSM
	B2GF-V14S	1.2%	4Ø16 steel	Steel links, S14,90°, two sides, NSM
	B2GF-D20S	1.2%	4Ø16 steel	Steel links, S20,45°, two sides, NSM
	B2GF-V20F	1.2%	4Ø16 steel	GFRP links, S20,90°, two side, NSM
	B2GF-D20F	1.2%	4Ø16 steel	GFRP links, S20,45°, two side, NSM
3	B2GF-U20F	1.2%	4Ø16 steel	GFRP double-C warp stirrups, S20,90°, NSM
	B2GF-20PsF	1.2%	4Ø16 steel	GFRP Full warp stirrups, S20,90°, NSM
	B2GF-EV20F	1.2%	4Ø16 steel	GFRP strips, s20, w10, EBR
4	B2GF-Sb1	1.2%	4Ø16 steel	GFRP bent bar, one/face, NSM
	B2GF-Sb2	1.2%	4Ø16 steel	GFRP bent bar, two/face, NSM
	B2GF-Sb1- EV20F	1.2%	4Ø16 steel	GFRP bent bar, one/face, NSM, with GFRP strips, EBR
	B2GF-Sb2- EV20F	1.2%	4Ø16 steel	GFRP bent bar, two/face, NSM, with GFRP strips, EBR

Table 2 Concrete mix design for cubic meter

Mix name	Cement (kg/m^3)	W/C	Sand (kg/m^3)	Gravel (kg/m^3)	*Vgf*, %	SP/C	Super-plasticizer (kg)
NC	350	0.5	620	1240	0	0	-
FC-0.6%	350	0.5	620	1240	0.6	0.01	3.5
FC-1.2%	350	0.5	620	1240	1.2	0.01	3.5

W/C: the ratio of water to cement; *Vgf*: the volume fraction of glass fiber; SP/C: the ratio of Super-plasticizer to cement.

techniques for GFRC beams were summarized in Table 1.

2.2 Materials properties

2.2.1 Concrete

Three mixes were used in this research as mentioned in Table 2. The actual compressive strength was 25 MPa for normal concrete and 27 and 29 MPa for GFRC with fiber ratios of 0.6% and 1.2%, respectively.

The straight-end shape discrete glass fibers used in the concrete mix according to the manufacturer were as follows:

-Glass fiber length=24 mm-young's modulus=5 GPa, -ultimate tensile strength=2000 MPa, -Fiber Density=2.5×10^{-5} N/mm^3 -ultimate tensile strain=2.2%.

2.2.2 Steel bars

The longitudinal steel used for beams reinforcement and the steel links used in external strengthening had a yield strength of 366 MPa and a modulus of elasticity of 200 GPa.

2.2.3 GFRP sheets

The glass fiber used in specimens had an ultimate strength of 1480 MPa, an elasticity modulus of 70 GPa, an ultimate elongation of 2.1%, and had an effective thickness of 0.17 mm, 500 mm width, and about 5000 mm length.

μ:fiber ratio in concrete; AS: reinforcing area of steel reinforcement bars in tension; S.S: strengthening systems on the outer surface of the beam

All specimens have only stirrups outside two supported in the respective overhang length, with 40 mm spacing.

B0, B1, and B2 refer to the ratio of GF of 0.0, 0.6, and 1.2%, respectively.

S1, and F1, refer to the materials of main reinforcement Steel and Fiber, respectively.

V, and D, refer to the direction of strengthening links vertical and diagonal with 45°.

20, and 14, refer to the distance between strengthening links, bars, and strips in cm from center to center.

S, and F, refer to the materials of strengthening Steel and Fiber, respectively.

U, Ps, and E refer to the strengthening technique of NSM double-C, NSM Full warp, and EBR strips, respectively. Knowing that PsF: GFRP strip rounded to be a bar (strips with 100 mm width).

Sb1, and Sb2, refer to the number of GFRP bent-up bars on each side.

2.2.4 GFRP bars

The GFRP bars with 16 mm diameter are used as main reinforcement for three beams in group 1. Links with 10 mm diameter are used in the strengthening of beams. The mechanical properties of the GFRP bars used in this study are presented in Table 3.

2.3 FRP and steel strengthening systems

2.3.1 Installation of NSM GFRP and steel (links or bars as stirrups)

The grooves cut into the concrete beam's surface were both about 10 mm wide and 10 mm deep with different lengths depending on the shape of strengthening used. Fig.

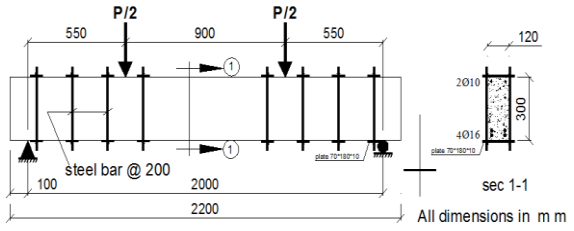

(a) GFRC beams B2GF-V20S

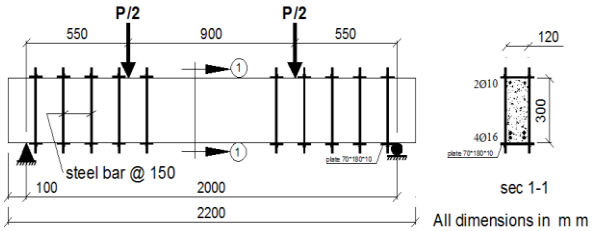

(b) GFRC beams B2GF-V14S

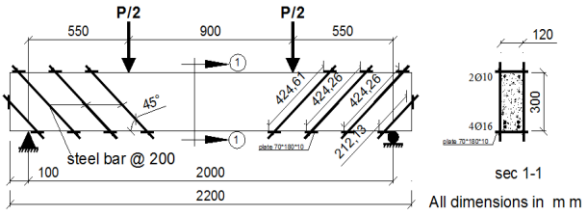

(c) GFRC beams B2GF-D20S

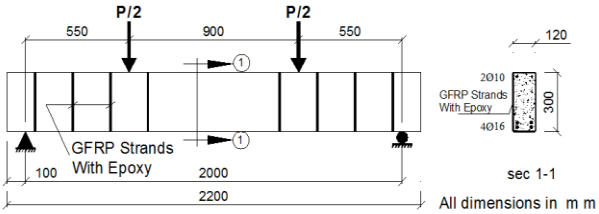

(d) GFRC beams B2GF-20Ps

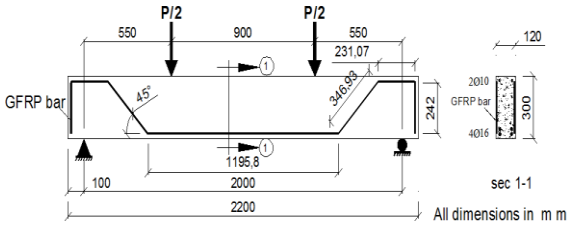

(e) GFRC beams B2GF-Sb1

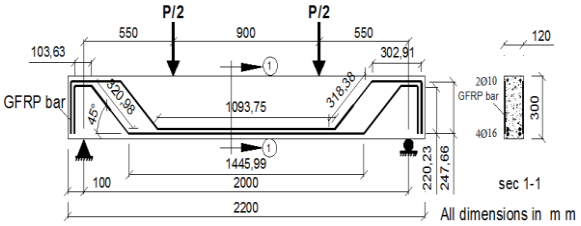

(f) GFRC beams B2GF-Sb2

Fig. 2 Various strengthening techniques of NSM GFRP and steel for GFRC beams

(a) Vertical and inclined grooves

(b) bent up grooves

Fig. 3 Grooves carved through the concrete beam's surface

(a) Vertical bars at 200 mm spacing.

(b) Vertical bars at 140 mm spacing

(c) Inclined bars (45°) at 200 mm spacing measuring at bottom of the beam

Fig. 4 Strengthening preparation of NSM steel bars

2 shows various NSM strengthening systems for GFRC beams. To install the NSM elements; firstly, a collection of grooves of specific dimensions carved through the concrete cover of the specimens as shown in Fig. 3. Secondly, ensure good bonding between the epoxy adhesive and the concrete.

Thirdly, for steel bars, insert steel bars into grooves by passing through perforated two plates, one of the above and the other in the bottom of the beam. Then, Interlock Nuts into Threaded bars as shown in Figs. 4, and 5. For GFRP bars, the adhesive was added to the groove until filled fully. The GFRP bars were then placed into the grooves ensuring that they were fully coated with epoxy and the surface of

Table 3 Dimensional and mechanical properties of GFRP bars

Property	GFRP bars	
diameter of bars (mm)	16	10
area of bars (mm^2)	201	78.5
area of fibers (mm^2)	78.39	30.19
fiber ratio by area	39%	38.46%
tensile strength (N/mm^2)	1390	670
modulus of elasticity (N/mm^2)	76000	60000
elongation at failure	2.50%	2.10%

Fig. 5 Install NSM steel bars in the laboratory

Fig. 6 Strengthening preparation of NSM Inclined GFRP bar

the beam was smoothly finished as shown in Fig. 6. For GFRP bars as stirrups shaped from the sheet for beam (B2GF-20PsF), Strip 100 mm width cut from the sheet, put epoxy on it, then roll the strips to be bar Shaped easily. Finally, the strips wrapped around the cross-section of the beam on space 200 mm.

2.3.2 Installation of externally bonded GFRP strips

The surface of the GFRC specimens was prepared to form a strong bond by smoothing and turning around the sharp corners, coating the surface with a uniform thin film of two-component epoxy adhesive. Then, The FRP strips were pushed onto the underlying layer of epoxy position on the concrete surface. The strips were subjected to consistent pressure across their length to achieve a strong bond with concrete and cured specimens in the laboratory. Figs. 7, 8, and 9 show EB strengthening systems used for GFRC beams.

2.4 Test setup and ınstrumentation

All specimens were tested as simply supported under four-point loading with an effective span of 2000 mm between two supports and loaded with two equal point loads with 900 mm between the two loading points at 550 mm from each support. Loads were applied using a hydraulic jack with a Digital Load cell. All beams were tested up to failure under an incremental loading procedure. also, Cracks and the mode of failure were observed. The tests were conducted using three different types of instruments: a linear variable differential transformer (LVDT), strain gauges, and a load cell. Three electric dial gauges (LVDT) were placed at the bottom of beams to evaluate vertical displacements in the middle span of beams and the two others under two-point applied load. An

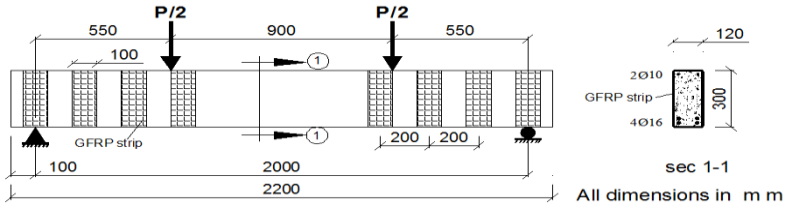

Fig. 7 Strengthening techniques of externally bonded GFRP strips for GFRC beams B2GF-D20S

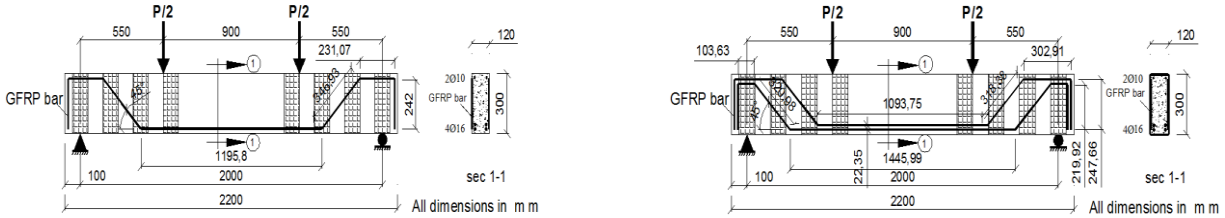

(a) GFRC beams B2GF-Sb1- EV20F (b) GFRC beams B2GF-Sb2- EV20F

Fig. 8 Description of NSM GFRP bars and externally bonded GFRP strips for GFRC beams

Fig. 9 Strengthening preparation of Beam B2GF-EV20F used externally bonded GFRP strips

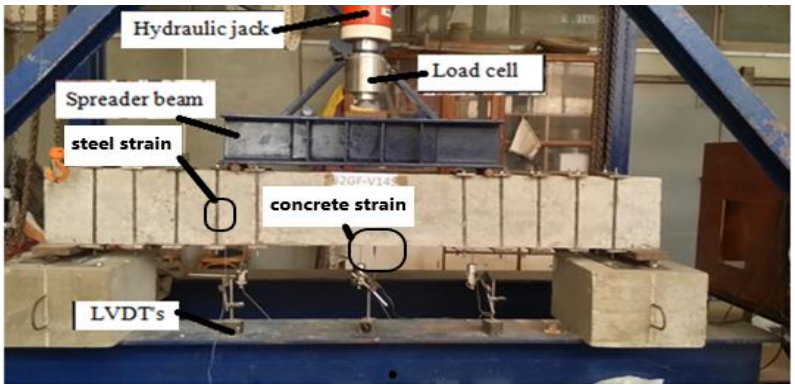

Fig. 10(a) The photograph of the Specimens before the test

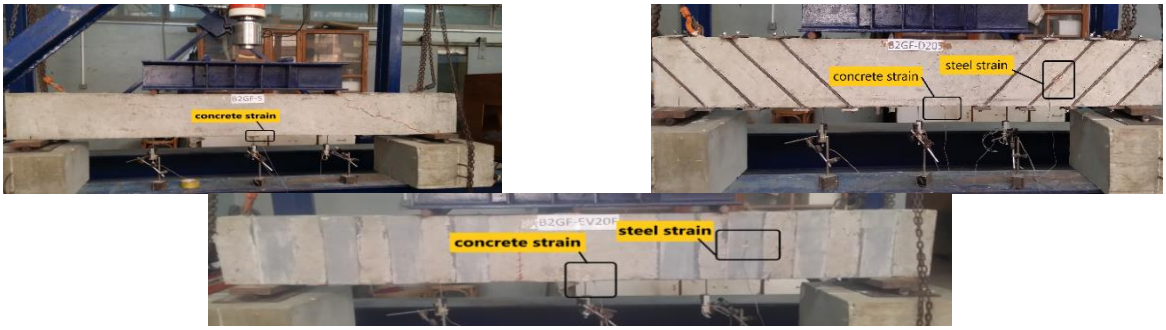

Fig. 10(b) the positions of the electrical strain gauges

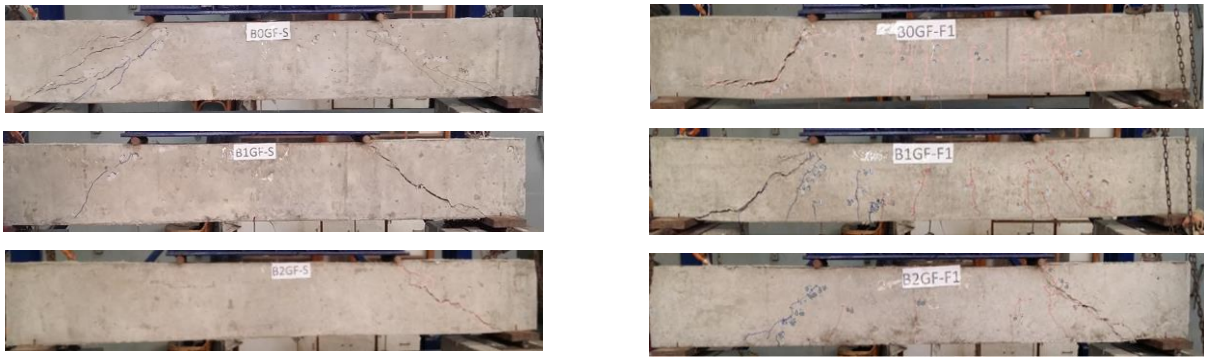

(a) Beams reinforced with steel bars (b) Beams reinforced with GFRP bars

Fig. 11 The crack pattern of shear failure for all tested beams in the first group

electrical concrete strain gauge was applied for all beams to measure the concrete strains at the bottom face of the mid-span section. In all beams at group 2,3,4, an electrical steel strain gauge was attached directly to one of the steel bars, GFRP bars, or GFRP strips to evaluate the strain of shear strengthening during loading for each specimen. For beams strengthened with FRP bent up bars and strips, the strain gauges were fixed for each technique (one on bar and one on strip). Fig. 10(a) shows the photograph of the test setup. Fig. 10(b) shows the positions of the electrical strain gauges.

3. Experimental results and discussions

The readings from the crack load, ultimate load of shear strength, displacements, and the strain of concrete, steel strengthening bar, GFRP strengthening bar, and GFRP strengthening sheet were recorded. These results are summarized in Table 4.

3.1 Cracking and mode of failure

All the beams were tested till failure due to diagonal shear cracking in the region of maximum shear. The failure mode of all the specimens was a shear failure and the orientation of the diagonal shear crack was approximately from support to concentrated point of loading. In the first group, The GFRC beams reinforced with steel bars without strengthening failed when the initiation of the splitting cracks appeared then the load dropped slightly after reaching the ultimate load with increasing deflection. In the case of beams reinforced with GFRP bars, larger deflection and crack width formed with increasing load until sudden

Table 4 Summary of test results

Group no.	specimen	load			deflection		measurements				Failure mode
		P_y (kN)	P_u (kN)	P_u/P_u control	Δy (mm)	Δu (mm)	Δu control (mm)	k (kN/mm)	I (kN.mm)	DF	
1	B0GF-S1	65	85.5	-------	6	8.4	--------	10.83	718.2	1.40	Shear failure
	B1GF-S1	87	101	1.18	6	8.8	--------	14.50	888.8	1.47	Shear failure
	B2GF-S1	101	109	1.27	6	9.2	9.2	16.83	1002.8	1.53	Shear failure
	B0GF-F1	80	91	-------	11.3	14.2	--------	7.08	1292.2	1.25	Shear failure
	B1GF-F1	90	108	1.18	11.7	15.1	--------	7.7	1630.8	1.29	Shear failure
	B2GF-F1	103	116.8	1.28	11.9	16	11.9	8.65	1868.8	1.34	Shear failure
2	B2GF-V20S	115	140	1.28	6.3	12.6	4.6	18.25	1764	2.00	Shear failure
	B2GF-V14S	130	184	1.44	6.2	15.4	4.8	20.97	2833.6	2.48	Shear failure
	B2GF-D20S	125	157	1.68	6.1	13.9	4.3	20.49	2182.3	2.28	Shear failure
	B2GF-V20F	120	141	1.29	6.9	12.9	4.7	17.39	1818.9	1.87	Shear failure followed by debonding
	B2GF-D20F	130	158	1.45	7	14.1	4.4	18.57	2227.8	2.01	Shear failure followed by debonding
3	B2GF-U20F	122	155	1.42	5.4	12	4.3	22.59	1860	2.22	Shear failure followed by debonding
	B2GF-20PsF	122	195	1.79	5.5	12	4.2	22.18	2340	2.18	Shear failure followed by debonding
	B2GF-EV20F	105	217	1.99	4.7	10.7	4.1	22.34	2321.9	2.28	Shear failure followed by debonding
4	B2GF-Sb1	107	142	1.30	5.5	9.1	5.3	19.45	1292.2	1.65	Shear failure followed by debonding
	B2GF-Sb2	100	155	1.42	4.3	8.2	4.7	23.26	1271	1.91	Shear failure followed by debonding
	B2GF-Sb1-EV20F	115	221	2.03	4.2	9.9	3.8	27.38	2187.9	2.36	Shear failure followed by debonding
	B2GF-Sb2-EV20F	120	240	2.20	4.3	11	3.7	27.91	2640	2.56	Shear failure followed by debonding

Where; P_y: Load at yield, P_u: Ultimate load, Δy: Deflection at P_y, Δu: Deflection at P_u,
$P_u/P_{u\ control}$: Ultimate load of beam/Ultimate load of the control beam, $\Delta_{u\ control}$: Deflection at Ultimate load (P_u) for control beam (B2GF-S1), K: Initial stiffness, I: Energy Absorption, DF: Ductility factor.

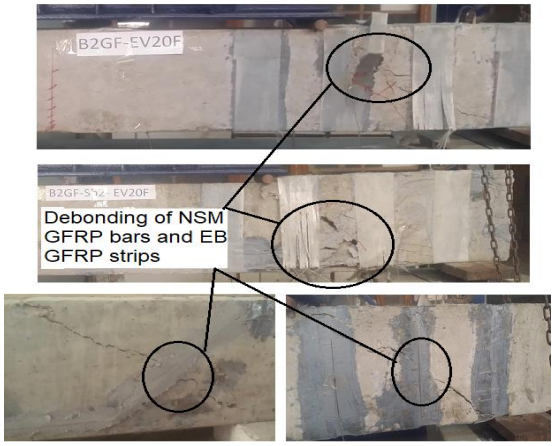

Fig. 12 The debonding shear failure beam by steel links

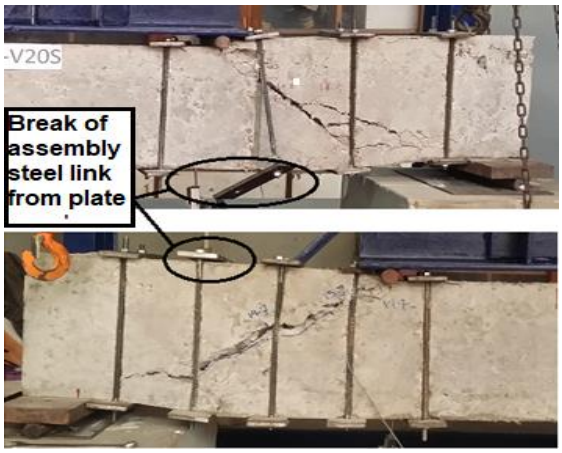

Fig. 13 The shear failure for strengthened

brittle rupture with loud sound occurred at ultimate load, then the load dropped suddenly with a very small increase in deflection. Fig. 11 shows the progress of the crack pattern that led to shear failure in all the tested beams in the first group. The beams strengthened with GFRP bars or sheets at the shear region failed by the diagonal tension followed by partial premature de-bonding (delamination between GFRP and concrete) or separation of GFRP bars or sheets due to strong interface shear stresses at this position at the end of the FRP and ripping off some strengthening elements. Fig. 12 shows the pattern of shear failure of these specimens. Beams externally strengthened by the steel links were failed by the diagonal shear crack behind steel links followed by failure of the assembly as shown in Fig. 13. The diagonal crack of the strengthened beams occurred at a relatively greater load than for the control beam (B2GF-S1). Table 4 summarizes the modes of failure for the tested specimens.

3.2 Load-deflection behavior

3.2.1 Effect of volume of glass fiber on shear behavior of beams

Figs. 14 and 15 show the load- span deflection relationship for different glass fiber ratios (0, 0.6%, and 1.2%) for group 1. Fig. 14 shows the first three specimens

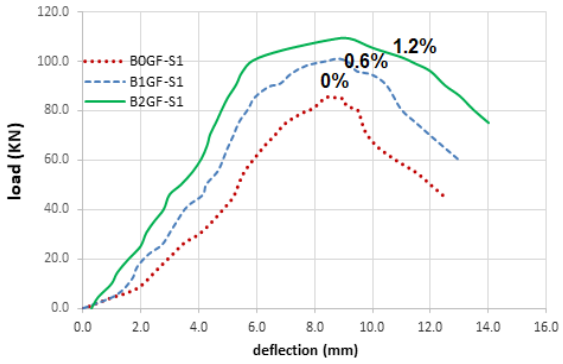

Fig. 14 The Load-Deflection curve for the steel-reinforced beams in Group 1

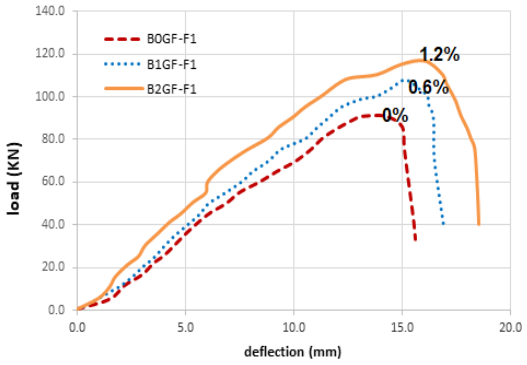

Fig. 15 The Load-Deflection curve for the Glass fiber-reinforced beams in Group 1

reinforced with steel bars as main reinforcement, and Fig. 15 shows the second three specimens reinforced with glass fiber bars as main reinforcement. Both figures show increasing in the ultimate load and decreasing in the deflection for the beams with glass fiber compared to normal concrete beams (0% glass fiber). As The first three specimens in group 1, GFRC beams with fibers 0.6% and1.2% led to an increase in ultimate load by 18.1% and 27.5%, respectively, and a slight increase in ultimate deflection by 4.7% and 9.5%, respectively. From the second three specimens in group 1, adding discrete glass fiber by 0.6% and 1.2% led to an increase in the ultimate load by 18.7% and 28.4%, respectively, and ultimate deflection increases slightly by 6% and 12.6%, respectively. The beams (B0GF-S1) and (B0GF-F1) without glass fiber in concrete showed lower stiffness and ductility than GFRC beams had (0.6, and1.2%) glass fiber in concrete as shown in Table 4.

The relation between fiber content and failure load with a different type of the main reinforcements (steel, GFRP) is shown in Fig. 16. From the results, the failure was brittle because there are no stirrups in the critical shear zone of beams, the presence of stirrups minimizes the danger of the sudden and brittle type of shear failure, but the presence of glass fibers increased the ductility due to the glass fibers have high values of tensile strength and also, increase the modulus of elasticity and the tensile strength of concrete (Abdul-Zaher *et al*. 2016). It was noticed that by increasing glass fiber ratio, the values of the concrete tensile strength,

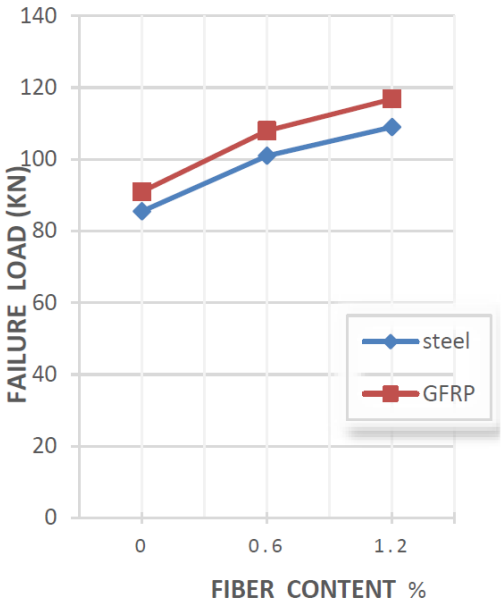

Fig. 16 The relation between fiber content and failure load f or Group 1

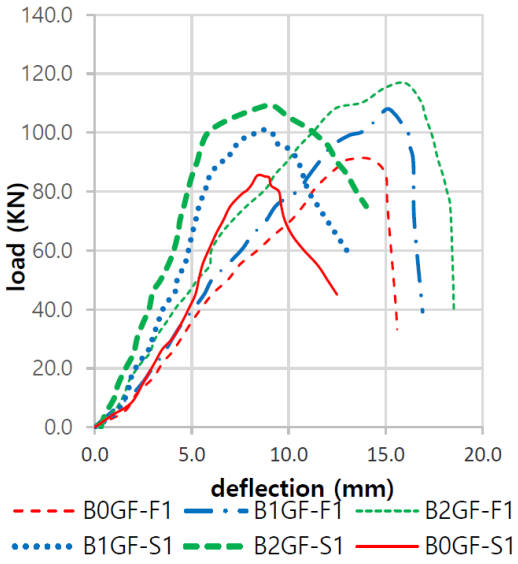

Fig. 17 The Load-Deflection curve

shear strength, first cracking load, the ultimate shear capacity, modulus of elasticity, and maximum deflection increased. On the other hand, the number and width of cracks decreased because fibers transfer tension across diagonal cracks In FRC beams, and consequently control the opening of diagonal cracks. The values of the deflection at a certain load (Δu control) decreased, and consequently, the stiffness of the RC beams was enhanced.

3.2.2 Effect of main reinforcement materials (steel-GFRP bars)

The effect of using GFRP bars in reinforcement could be observed from the shear behavior of specimens B0GF-F1, B1GF-F1, and B2GF-F1 in group 1 and comparing it with specimens B0GF-S1, B1GF-S1, and B2GF-S1 in group 1, as shown in Fig. 17. Using the longitudinal GFRP

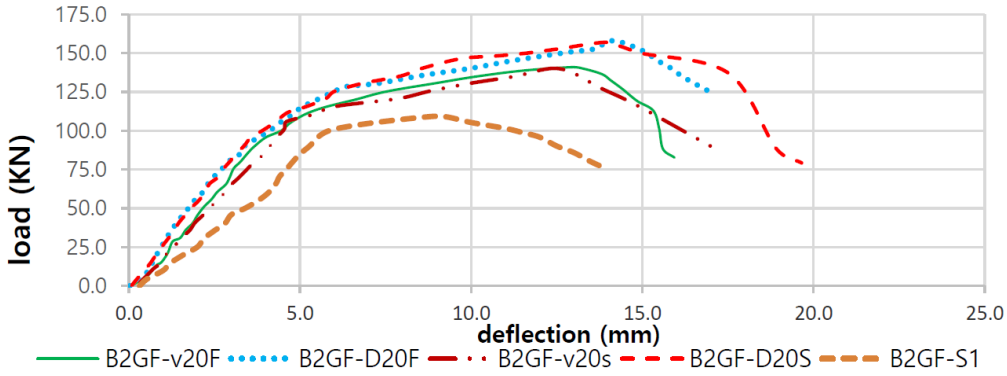

Fig. 18 The Load-Deflection curve for Group 2

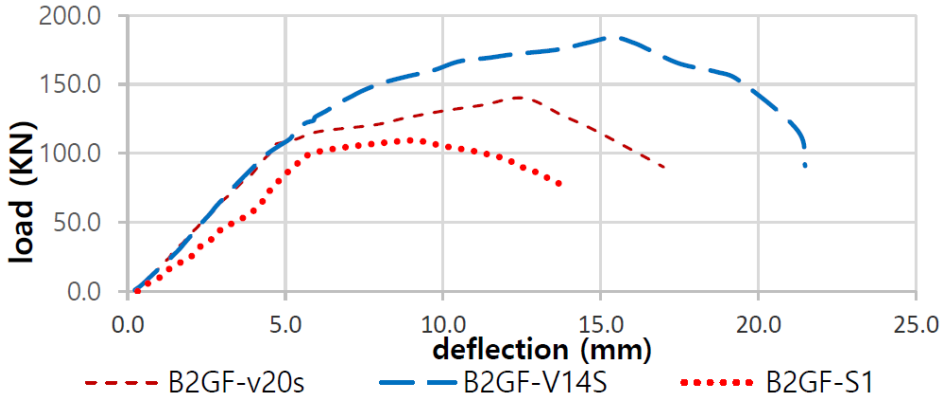

Fig. 19 The Load-Deflection curves for Group 2

reinforcement led to a slight improvement in the shear capacity of GFRC beams without stirrups (Raid *et al*. 2016). The ultimate load was greater than that of specimens using traditional steel reinforcement by 6.4%, 6.9%, and 7.2% using fiber ratios of 0, 0.6%, and 1.2%, respectively. However, the deflection was increased at the same load level in specimens with steel reinforcement. The results show that using GFRP bars instead of traditional steel bars as main reinforcement increased slightly the ultimate load because of the higher tensile strength of GFRP bars (Raid *et al*. 2016), also present a high level of deformability at beam failure, but decreased ductility, and stiffness (higher deflections) as a result of the lower modulus of elasticity of GFRP bars as compared to steel bars (Raid *et al*. 2016). The beams reinforced with GFRP bars do not yield and provide a linear-elastic behavior until brittle tensile failure, larger deflections, and wider cracks occur before failure because of their low modulus of elasticity. When GFRP bars are used, a balance between serviceability and strength should be considered.

3.2.3 Effect of strengthening materials (steel-GFRP links)

The effect of strengthening materials (steel links-GFRP links) could be noticed from the behavior of beams (B2GF-V20S and B2GF-V20F) having vertical links and (B2GF-D20S and B2GF-D20F) having inclined links as SNSM stirrups technique. Both materials improved the shear behavior in comparison with the control beam (B2GF-S1), where shear capacity was increased, and the deflection at the same loading level was decreased. Also, ductility, modulus of elasticity, toughness, and stiffness were increased as shown in Fig. 18. The ultimate load was increased by 28.4% and 29.4% for beams strengthened by SNSM vertical steel and GFRP links, respectively. Also, SNSM diagonal steel and GFRP links increased ultimate load by 44% and 45%, respectively compared to the control beam (B2GF-S1).

The results show that using GFRP links instead of steel links in the strengthening technique increased slightly the ultimate load because of the higher tensile strength of GFRP links but decreased ductile behavior as a result of the lower modulus of elasticity of GFRP links.

3.2.4 Effect of links orientation (vertical-45° inclined links)

The effect of links inclination (90° vertical links-45° inclined links) could be noticed from the behavior of beams (B2GF-V20S and B2GF-D20S) with steel strengthening and (B2GF-V20F and B2GF-D20F) with GFRP strengthening as SNSM stirrups technique. Both inclinations improved the shear behavior in comparison with the control beam (B2GF-S1). Where the ultimate load was increased, and the deflection at the same loading level was decreased. As a result, ductility, modulus of elasticity, and stiffness were increased as shown in Fig. 18. The ultimate load was increased by 12.1%, and 12% when used 45° inclined steel links, and fiber links, respectively instead of 90° vertical links. From the results, the study proved that the use of 45° inclined links enhanced the ultimate load,

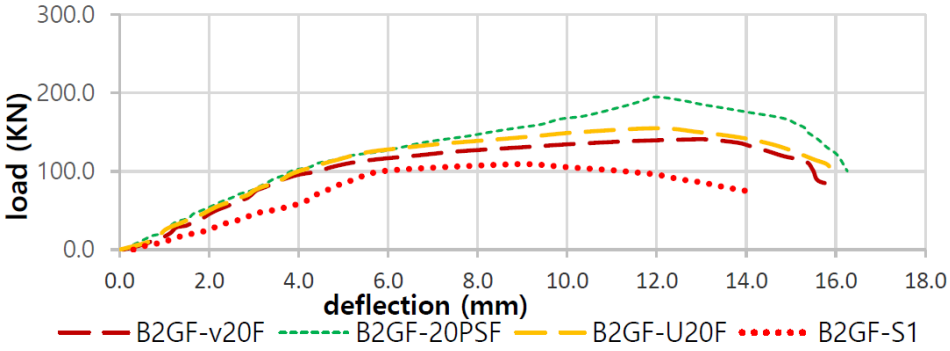

Fig. 20 The Load-Deflection curves for Group 3

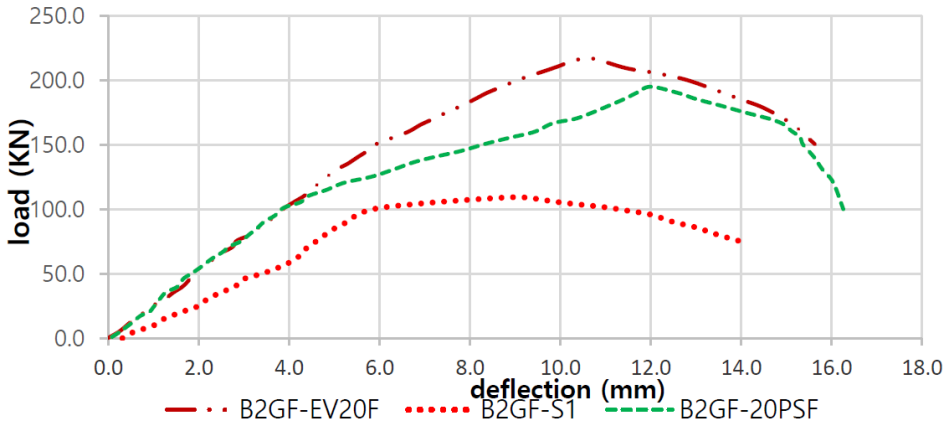

Fig. 21 The Load-Deflection curves for NSM and EBR technique

shear capacity, and ductility of the reinforced concrete beams despite installation difficulty. The inclined links work better than the vertical links in resisting the shearing forces and restraining the shear stresses formation in the RC beam because the orientation of inclined links is almost perpendicular to the diagonal shear cracks in shear zones. Therefore, the use of inclined links is an effective technique to enhance the shear capacity of the reinforced concrete beam. The deflection values of the RC beam with 45° inclined links are less than the RC beam with vertical shear links at the same applied load, the difference in deflection may be due to the stiffness which is a slope of the load-deflection curve of the beam.

3.2.5 Effect of spacing between steel links.

Reducing the link spacing from 200 mm in strengthened beam B2GF-V20S to 140 mm in beam B2GF-V14S led to an increase in the ultimate capacity of the beam by 31.4% as shown in Fig. 19 and Table 4. The load-carrying capacity of those two beams was higher by 28.4 % and 68.8% compared to the control beam (B2GF-S1).

From the figure, it is evident that decreasing in spacing between web reinforcement by increasing the number of stirrups increased the ultimate load and reduced the deflection at the same load and consequently, the ductility, stiffness, and toughness of the specimen were increased. Increasing the number of shear reinforcement showed a clear effect in controlling the crack width and contribute to the behavior of the shear mechanism by improving the contribution of the dowel action and limiting the opening of inclined shear cracks, thus enhancing shear transfer by aggregate interlock.

3.2.6 Effectiveness of SNSM links technique and NSM FRP stirrups shape

The load-deflection at mid-span relationships for strengthened specimens with SNSM links (B2GF-V20F), NSM FRP double-C stirrups (B2GF-U20F), NSM GFRP transverse stirrups around cross-section (box shape or full wrap) (B2GF-20PsF), and control beam (B2GF-S1) are shown in Fig. 20. These relationships indicate that using NSM GFRP transverse stirrups around the cross-section led to the highest improvement in the shear strength compared to other techniques. The ultimate strength for beams B2GF-V20F, B2GF-U20F, and B2GF-20PsF increased by 29.4, 42.2, and 78.9%, respectively compared to the control beam. The results show that the SNSM links technique at two sides of beams exhibits a lower increase in strength and higher deflection because of de-bonding of GFRP at failure because of the cut-out in the fiber link. In contrast, when using double-C shaped or closed stirrups on four faces of a beam, more increase in strength and lower deflection resulted. Changing the shape from full wrap stirrups confining the cross-section as in beam (B2GF-20PsF) to link as in beam (B2GF-V20F) or double-C-shape as in beam (B2GF-U20F) led to a decrease in the ultimate load by 27.7, and 20.5%, respectively, and increase in the ultimate deflection by only 7.5% for links and almost zero for double-C-shape. These results indicate that the most effective strengthening is obtained when using the full

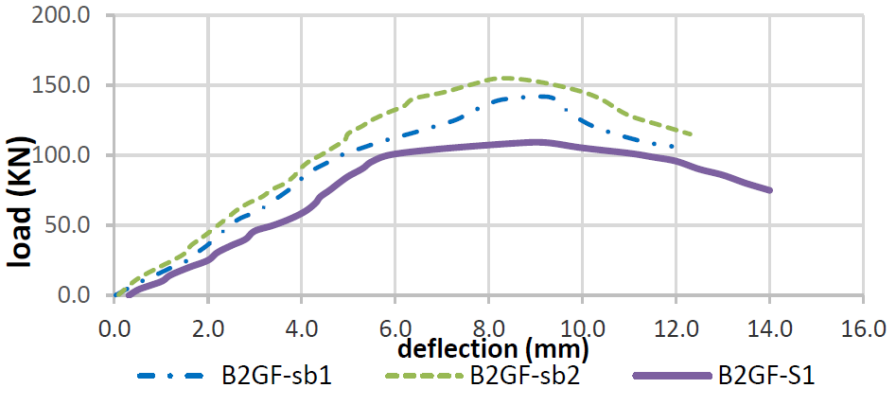

Fig. 22 The Load-Deflection curves for Group 4

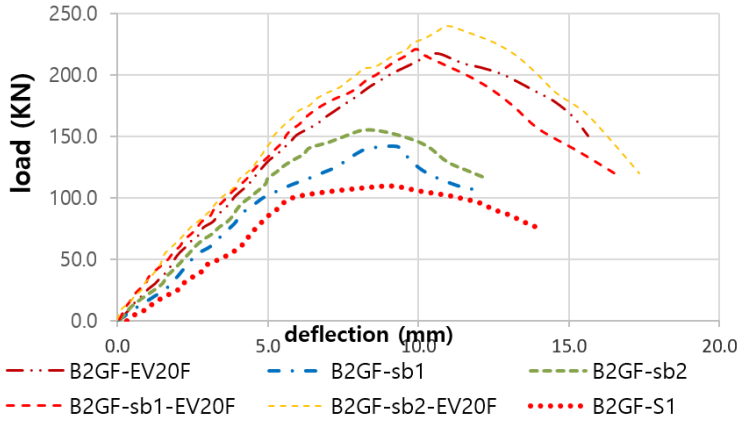

Fig. 23 The Load-Deflection curves for Group 4

stirrups (complete wrapping). Furthermore, the load-deflection behavior was improved by using the NSM GFRP transverse stirrups and significantly increased in the ductility, and bond strength because of the increase in bonding by increasing anchored.

3.2.7 Technique of NSM bars twisted from strips and EBR of the same strips

The effectiveness of EBR and NSM techniques in increasing the shear resistance of GFRC beams can be seen through the behavior of beams B2GF-EV20F and B2GF-20PsF, respectively as shown in Fig. 21. When compared with the control beam (B2GF-S1), the two beams B2GF-EV20F and B2GF-20PsF had an increase of 99% and 78.9% in the ultimate load, respectively. NSM technique attained a significant increase in the maximum load. also, the ultimate load decrease by 20.3% about EBR techniques. EBR strips techniques decrease maximum deflection than NSM bars Twisted from the same strips. The NSM bars and EBR strips limited shear cracks width development due to an important aggregate interlocking action. In NSM Technique, the amount of site installation work decreased because grooves cut into the concrete cover instead of longer surface preparation, The FRP is well attached to the concrete, avoid de-bonding failures, The FRP bars are protected by the concrete cover from damage due to impact, fire, and other causes. But, EBR Technique has the sensitivity to fire and vandalism, as well as the longer time required to prepare the beam zones for the FRP bond, which it considers apart from the relatively high expense of the FRP systems. But EBR techniques increased the ultimate load and decreased maximum deflection than the NSM technique in this paper because the strip covers more surface area than the bar. So, using strips in both techniques will be recommended in the future work subject to be investigated by the authors.

3.2.8 Effect of NSM GFRP bent bars technique

Bent bars were applied using the NSM technique for shear strengthening of beams through one or two bent GFRP bars on each side of beams (B2GF-Sb1) and (B2GF-Sb2), respectively. The bars are bent up at 45° along the outer length of beams. The load-deflection behavior of these beams is shown in Fig. 22. The ultimate load increased by 30.3%, and 42.2% for beams B2GF-Sb1, and B2GF-Sb2, respectively, and the mid-span deflection at maximum load was decreased by 1%, and 11%, respectively compared with the control beam (B2GF-S1). The number of bent-up bars does not affect the behavior of beams significantly, only the presence of the bars increased the shear resistance as expected. Where the bent-up bars are needed to resist bending moment, the inclined legs of bent-up bars resist diagonal tension and the shear strength in the region of high shear by crossing the diagonal shear cracks.

3.2.9 GFRP strips, GFRP bent-up bars, and GFRP bent bars with GFRP strips together

In this part, five shear strengthening systems were

studied and compared.

1- External Bonded transverse GFRP strips 10 cm wide around cross-section by EBR technique (B2GF-EV20F) every 20 cm from center to center,

2- One bent GFRP bars by NSM technique (B2GF-Sb1),

3- Two bent GFRP bars by NSM technique (B2GF-Sb2),

4- A combination of first and second techniques (B2GF-Sb1- EV20F),

5- A combination of the first and third techniques (B2GF-Sb2- EV20F).

This parameter's effect may be noticed from the behavior of five specimens (B2GF-EV20F, B2GF-Sb1, B2GF-Sb2, B2GF-Sb1- EV20F, and B2GF-Sb2- EV20F), respectively in compared with control beam (B2GF-S1) as shown in Fig. 23. Using the five-technique led to a significant increase in the shear strength, stiffness, toughness, and ductility of the strengthened beams compared to the control specimen, especially the fifth technique. In addition, five strengthened specimens had lower deflection values at the same loading level compared to control specimens without strengthened. On the other side, for the five-strengthening technique, the ultimate load increased by 99%, 30.3%, 42.2%, 103%, and 120% compared to the control beam. And, the mid-span deflection decreased by 53.3 %, 38%, 46.7 %, 55.4%, and 57.6%. The large improvement for shear strengthening is shown in Fig. 23. This result shows that the SNSM bent bars and EBR strips form a good combination strengthening to resist applied load, redistribute the total stress onto the EBR strips and SNSM bent bars when the concrete beam is subjected, and increase the ductility, stiffness, and toughness of the beam. Due to better confinement to the concrete, the confinement of the bending in the main steel was reduced and the load-carrying capacity also increased. In the future, bent-up bars will be used along the beam with stirrups in strengthening to carry the applied shear forces.

3.3 Cracking and ultimate loads

The first cracking load and ultimate load values are shown in Table 4 for all specimens. Beam B2GF-Sb2-EV20F had the highest ultimate load relative to the control beam by about 120%. This is logical since this specimen had two types of GFRP strengthening (two bent bars and strips). The Increase in ultimate loads was accompanied by a significant increase in deflection.

3.4 Measurements from load-deflection curves

The following measurements can be assessed based on the load-deflection curves:

3.4.1 Initial stiffness (K)

The ratio of load at yield level (P_y) to corresponding displacement (Δy) can be used to calculate stiffness (K) (Said *et al*. 2020). The stiffness (K) for all beams has improved. For Group 1, compared (B1GF-S1, B2GF-S1) with (B0GF-S1) and compared (B1GF-F1, B2GF-F1) with (B0GF-F1), the stiffness was enhanced for B1GF-S1, B2GF-S1, B1GF-F1, and B2GF-F1 by 33.9%, 55%, 9%, and 22%, respectively. Accordingly, using discrete glass fiber concrete displayed an enhancement in the stiffness compared with normal concrete, and also by increasing the discrete glass fiber ratio from 0.6 to 1.2%, stiffness improved. For Group (2,3, and 4), the stiffness for all strengthened beams B2GF-V20S, B2GF-V14S, B2GF-D20S, B2GF-V20F, B2GF-D20F, B2GF-U20F, B2GF-20PsF, B2GF-EV20F, B2GF-Sb1, B2GF-Sb2, B2GF-Sb1-EV20F, and B2GF-Sb2- EV20F was higher than B2GF-S1by 8%, 25%, 21%, 3%, 10%, 34%, 32%, 33%, 16%, 38%, 63%, and 66%, respectively. The increase in the stiffness of the strengthened beams occurred due to the existence of strengthening material (steel and GFRP bars) which have a high modulus of elasticity.

3.4.2 Energy absorption (toughness)

The area under the load-deflection curve is defined as energy absorption (I). It is a function of ultimate load (P_u) and ultimate deflection (Δu) (Said *et al*. 2020). As a result, Energy Absorption can be a useful tool for assessing the ductility of beams. For Group 1, compared (B1GF-S1, B2GF-S1) with (B0GF-S1) and compared (B1GF-F1, B2GF-F1) with (B0GF-F1), the energy absorption was enhanced for B1GF-S1, B2GF-S1, B1GF-F1, and B2GF-F1 by 24%, 40%, 26%, and 45%, respectively. Accordingly, using discrete glass fiber concrete displayed an enhancement in the energy absorption compared with normal concrete, and by increasing the discrete glass fiber ratio, energy absorption improved. For Group (2, 3, and 4), compared with un-strengthened beam (B2GF-S1), a significant increase in the toughness was observed for all strengthened beams B2GF-V20S, B2GF-V14S, B2GF-D20S, B2GF-V20F, B2GF-D20F, B2GF-U20F, B2GF-20PsF, B2GF-EV20F, B2GF-Sb1, B2GF-Sb2, B2GF-Sb1-EV20F and B2GF-Sb2- EV20F by 76%, 183%, 118%, 81%, 122%, 85%, 133%, 132%, 29%, 27%, 118%, and 163%, respectively. The availability of a variable strengthening technique that provided more ductile behavior for the tested beams increased the toughness of the strengthened beams. Finally, Energy Absorption (the toughness) of the RC beams is enhanced by increasing discrete glass fiber ratio and strengthened beam.

3.4.3 Ductility Factor (DF)

Ductility refers to a member's ability to withstand inelastic deformations above yield without losing significant load energy. The load-deflection curve of the tested specimens was used to determine the ductility factor (DF) of the specimen. The ductility factor (DF) of the beam can be expressed based on the deflection of the beam, it can be calculated as the ratio [$\Delta u/\Delta y$] (Shanour *et al*. 2018), where Δu is the deflection at the ultimate level, and Δy is the deflection at the yield level. As shown in Table 4, the ductility value for all tested beams is indicated. In the first group, the ductility ratio increased with increasing the ratio of fiber in concrete mix and decrease when using GFRP bars as longitudinal main reinforcement instead of steel due to the brittle behavior of GFRP bars. In the second stage, the ductility factor increased as the result of using different strengthening systems on both sides of beams compared to

Table 5 Experimental concrete Strain of the Tested Beams in Group 1

Group no.	specimen	Fiber Ratio %	AS Bars	Strengthening Strain at Yield Level, (εy) (* 10-6 m/m)	Strengthening Strain at the Ultimate level, (εt) (* 10-6 m/m)	Strain Ductility, $\mu s=\varepsilon t/\varepsilon y$
1	B0GF-S1	0%	4Ø16 steel	575	675	1.17
	B1GF-S1	0.6%	4Ø16 steel	646	768	1.19
	B2GF-S1	1.2%	4Ø16 steel	676	830	1.23
	B0GF-F1	0%	4Ø16 GFRP	870	985	1.13
	B1GF-F1	0.6%	4Ø16 GFRP	900	1038	1.15
	B2GF-F1	1.2%	4Ø16 GFRP	915	1090	1.19

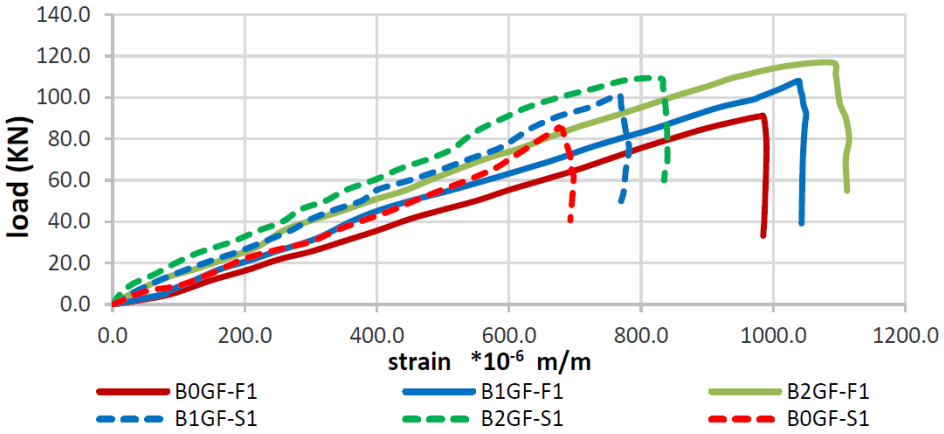

Fig. 25 The load-concrete strain relationships for tested beams in the first stage

the control beam, and this increase was more profound when using combined bent bars and external transverse strengthened technique by confining the cross-section in the shear zone.

The ductility increased when stirrups were applied all around the cross-section of beams in the shear zone compared to beams with links on both sides and the control beam (B2GF-S1). Also, when the number of external links was increased by decreasing their spacing between 200 mm to 140 mm, the ductility ratio increased by 24 %. Using GFRP longitudinal reinforcement and GFRP. The stiffness (K) for all beams has improved. Links in external strengthening instead of steel provided a slight decrease in ductility. Generally, the ductility of beams strengthened by EBR-GFRP strips in the shear zone with two external layers of bent bars (B2GF-Sb2-EV20F4) was higher than all strengthened beams. It was observed that the ductility ratio of strengthened beams (B2GF-V20S, B2GF-V14S, B2GF-D20S, B2GF-V20F, B2GF-D20F, B2GF-20PsF, B2GF-U20F, B2GF-EV20F, B2GF-Sb1, B2GF-Sb2, B2GF-Sb1-EV20F, and B2GF-Sb2- EV20F4) increased to about 31 %, 62 %, 49 %, 22%, 31%,45 %, 42%,49%, 8 %, 25 %, 54%, and 67 %, respectively compared the control beam (B2GF-S1).

3.5 Strain

3.5.1 Concrete strain

The behavior of beams and the quantity of concrete strain at the mid-span section on the bottom face of RC beams are explained by load-concrete strain curves. From the load- concrete strain curves, the strain ductility (μs) was defined as the ratio between strain in concrete at the ultimate level to the strain at the yield level ($\mu s=\varepsilon t/\varepsilon y$) (ACI Committee 318- 2014). Table 5 shows the concrete strain of all beams in Group 1 at the ultimate level (t), yield level (y), and strain ductility, $\mu s=\varepsilon t/\varepsilon y$.

The concrete strain and ultimate concrete strain for beams reinforced with (steel or GFRP bars) increased with the increasing proportion of glass fiber in the concrete mix due to the better load-carrying capability of beams as indicated in the load-concrete strain curves in Fig. 25. Due to the presence of fiber, concrete absorbs more energy and therefore improves its modulus of elasticity and tensile strength. However, at a certain load, increasing the proportion of glass fibers resulted in a decrease in concrete strain value. The addition of glass fibers by ratio 0.6% and 1.2% improved the concrete strain ductility of the tested beams by approximately 1.7% and 5.2%, respectively. The maximum concrete strain values for all beams were less than 0.002. According to the results, the ultimate concrete strains of beams reinforced with steel bars are lower than those of beams reinforced with GFRP bars, and the development of strain is also shown to be slower. The strain ductility ratio of GFRP-reinforced beams is lower than that of steel-reinforced beams due to the lower modulus of elasticity of GFRP bars and the brittle behavior of GFRP bars.

3.5.2 Strain in steel and GFRP strengthening

The shear strains of the steel bars, FRP bars, and FRP strips at the ultimate level (εt) and Yield Level, (εy) were recorded in Tables 6, 7 for Groups 2, 3, and 4. The strain ductility (s) was determined as the ratio of strain in the strengthening bars and strips at the ultimate level to strain at the yield level ($\mu s=\varepsilon t/\varepsilon y$) (Said *et al*. 2016) based on the

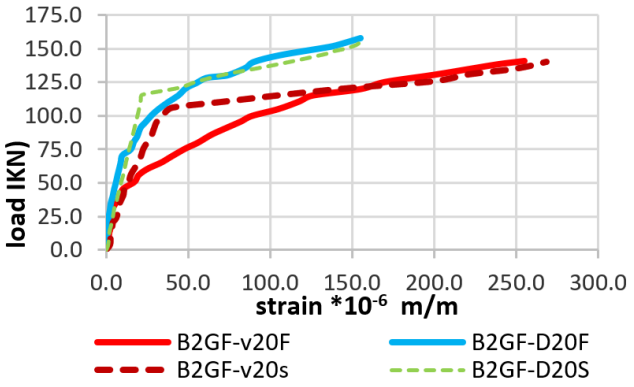

Fig. 26 The load-concrete strain relationships for tested beams in Group 2

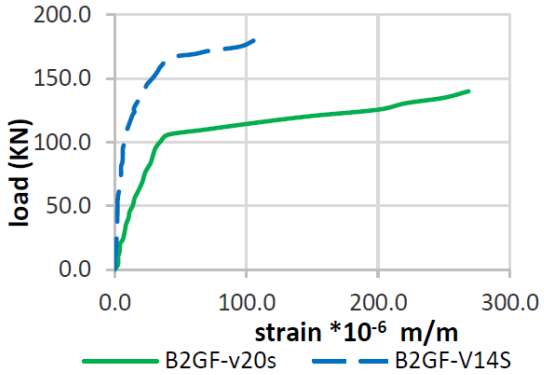

Fig. 27 The load-concrete strain relationships for some tested beams in Group 2

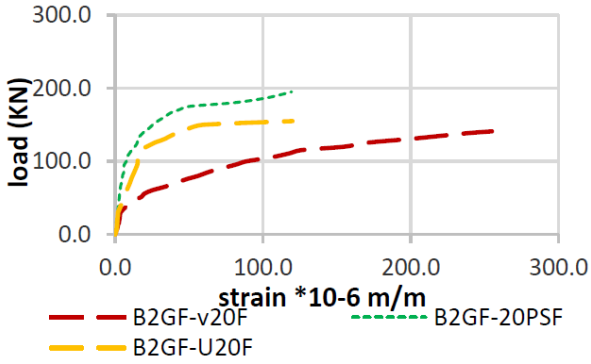

Fig. 28 The load-concrete strain relationships for some tested beams in Group 2, 3

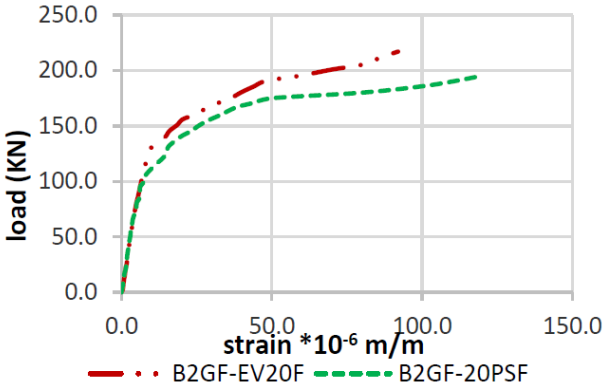

Fig. 29 The load-concrete strain relationships for some tested beams in Group 3

Table 6 Experimental concrete Strain of the Tested Beams in groups 2, 3, 4 which use one shear strengthening technique

Group no.	specimen	Strengthening systems (S.S)	Strengthening Strain at Yield Level, (εy) (* 10-6 m/m)	Strengthening Strain at the Ultimate level, (εt) (* 10-6 m/m)	Strain Ductility, $\mu s=\varepsilon t/\varepsilon y$
2	B2GF-V20S	Steel links, S20,90°, two sides, NSM	110	268	2.44
	B2GF-V14S	Steel links, S14,90°, two sides, NSM	16	114	7.13
	B2GF-D20S	Steel links, S20,45°, two sides, NSM	55	156	2.84
	B2GF-V20F	GFRP links, S20,90°, two sides, NSM	155	255	1.65
	B2GF-D20F	GFRP links, S20,45°, two sides, NSM	75	155	2.07
3	B2GF-U20F	GFRP double-C warp stirrups, S20,90°, NSM	23	120	5.22
	B2GF-20PsF	GFRP Full warp stirrups, S20,90°, NSM	14	119	8.5
	B2GF-EV20F	GFRP strips, s20, w10, EBR	7	92	13.14
4	B2GF-Sb1	GFRP bent bar, one/face, NSM	104	154	1.48
	B2GF-Sb2	GFRP bent bar, two/face, NSM	63	160	2.54

load- strengthening strain curves. Tables 6, 7 show the strain ductility (s) values that were expected.

The strain ductility of beams strengthened with steel and GFRP bars and strips were increased compared to un-strengthened beam B2GF-S1. The results indicate that employing GFRP links instead of steel links in the strengthening technique lowered ductile behavior due to the lower modulus of elasticity of GFRP links, as shown in Table 6. At the same applied load, the strain values of the RC beam with 45° inclined links are less than those of the RC beam with vertical shear links. The difference in strain could be due to stiffness, which is a slope of the load-strain curve of the beam as shown in Fig. 26. In addition, the strain ductility (s) of the RC beams is improved by employing 45° inclined links instead of vertical links, as indicated in Table 6. Because the distances between shear bars decreased by increasing the number of steel bars, the strain ductility for beam (B2GF-V14S) was larger than beam (B2GF-V20S), as mentioned in Table 6, and the strain at the same load was lowered as shown in Fig. 27. As may be seen in Fig. 28, The results indicate that using SNSM links (B2GF-V20F) on two sides of beams causes more strain than using double-C shaped (B2GF-U20F) or closed stirrups (B2GF-20PsF) on four faces of a beam at the same load due to GFRP de-bonding due to the cut-out in the fiber link and increased bonding by increasing anchored in closed

Table 7 Experimental concrete Strain of the Tested Beams in Group 4 which uses two strengthening techniques

			strips			Bent bars		
Group no.	specimen	Strengthening systems (S.S)	Strengthening Strain at Yield Level, (εy) (* 10-6 m/m)	Strengthening Strain at the Ultimate level, (εt) (* 10-6 m/m)	Strain Ductility, $\mu s=\varepsilon t/\varepsilon y$	Strengthening Strain at Yield Level, (εy) (* 10-6 m/m)	Strengthening Strain at the Ultimate level, (εt) (* 10-6 m/m)	Strain Ductility, $\mu s=\varepsilon t/\varepsilon y$
4	B2GF-Sb1-EV20F	GFRP bent bar, one/face, NSM, with GFRP strips, EBR	5.9	85	14.41	86	201	2.34
	B2GF-Sb2-EV20F	GFRP bent bar, two/face, NSM, with GFRP strips, EBR	5.2	90	17.31	70	200	2.86

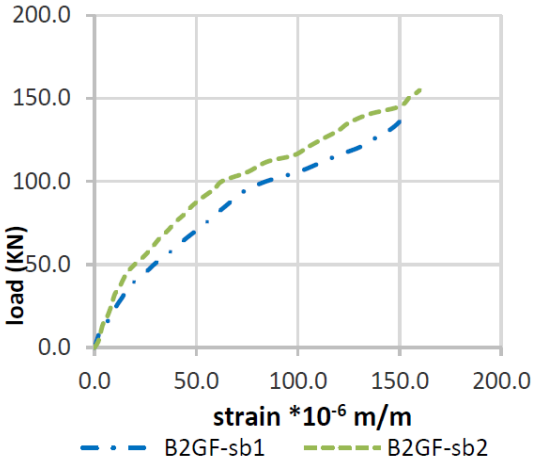

Fig. 30 The load-concrete strain relationships for some tested beams in Group 4

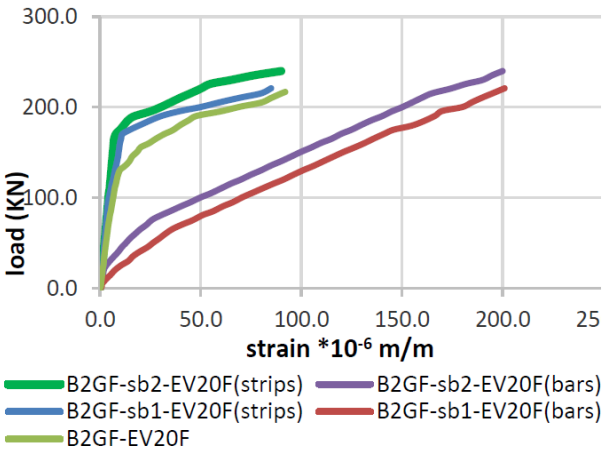

Fig. 31 The load-concrete strain relationships for tested beams in Group 4

stirrups. The shear strains on NSM bars and EBR sheets for B2GF-20PsF and B2GF-EV20F beams, respectively, were 119 and 92 um/m at ultimate load, indicating that EBR strips techniques reduce maximum strain more than NSM bar Twisted from strips. As demonstrated in Fig. 29.

The maximum shear strain increased as the number of bent-up bars increased and ductile behavior enhanced, as seen in Fig. 30 and Table 6. A strengthening technique (bent up bars) combined with strips increased maximum strain and strain ductility compared to using strips alone for shear strengthening beams, but reduced strain when compared to all other strengthening beams at a specified load, as illustrated in Fig. 31. The B2GF-Sb2- EV20F strengthened RC beam with GFRP sheet and bent bars has the highest maximum strain and strain ductility. As a result of the under-strengthening method, all beams have collapsed in a ductile way at the shear zone.

4. Analytical study

A shear strength formulation is proposed for GFRC beams without web reinforcement and strengthened with external shear reinforcement, either with NSM steel or GFRP bars, NSM GFRP bent up bars and EBR with GFRP strips. Design codes present formulation to calculate the shear strength of reinforced concrete beams with web reinforcement. There is no published formulation to calculate the shear strength of GFRC without web reinforcement, GFRP as main reinforcement, GFRP bent bars as external shear reinforcement.

The nominal shear resistance at the ultimate limit state, Vn, of GFRC beams can be expressed as

$$Vn = Vc + VS + Vf \quad (1)$$

Where: Vn: The shear capacity, Vc: Shear contribution of GFRC, Vs: Shear contribution of the external steel (links), Vf: Shear contribution of the external FRP (links, strips, bent bars).

4.1 Shear contribution of GFRC beams

4.1.1 Contribution of GFRC by using steel as longitudinal reinforcement

Zsutty (Hai *et al*. 2011) derived an equation for beams without web reinforcement including the effect of longitudinal steel reinforcement ratios (ρ), and the shear span to depth ratio (a/d). Ashour A (Hai *et al*. 2011) modified Zsutty's to account for the effect of fibers by introducing the parameter (F) to the equation

$$V_c = \left[\left(2.11\sqrt[3]{f_c'} + 7F\right)\sqrt[3]{\rho\frac{d}{a}}\right] \text{bd} \qquad \text{(N)} \qquad (2)$$

Where:

V_c : Shear prediction of glass fiber reinforced concrete for the steel-reinforced beams.

f_c' : Concrete cylinder compressive strength (MPa) and taken 0.85 characteristic cubes compressive strength (fcu).

F: Fiber factor $(L_f/D_f)V_{gf}d_f$

Where,

L_f: fiber length; D_f: Fiber diameter of steel fiber, in this paper, the equivalent of fiber diameter is used to proportion

Table 8 Comparison between Experimental and Theoretical Results

specimens	Experimental	proposed equations	
	$V_{n\,exp}$ (kN)	$V_{n\,ana}$ (kN)	$K1$
B0GF-S1	42.75	44.15	0.97
B1GF-S1	50.5	52.10	0.97
B2GF-S1	54.5	59.99	0.91
B0GF-F1	45.5	47.20	0.96
B1GF-F1	54	55.69	0.97
B2GF-F1	58.4	64.13	0.91
B2GF-V20S	70	65.09	1.08
B2GF-V14S	92	80.13	1.15
B2GF-D20S	78.5	79.62	0.99
B2GF-V20F	70.5	65.38	1.08
B2GF-D20F	79	80.02	0.99
B2GF-U20F	77.5	74.22	1.04
B2GF-20PsF	97.5	99.19	0.98
B2GF-EV20F	108.5	109.57	0.99
B2GF-Sb1	71	66.38	1.07
B2GF-Sb2	77.5	80.02	0.97
B2GF-Sb1- EV20F	110.5	135.57	0.82
B2GF-Sb2- EV20F	120	149.21	0.75
Kave			0.98

$K=V_{n\,exp}/V_{n\,ana}$

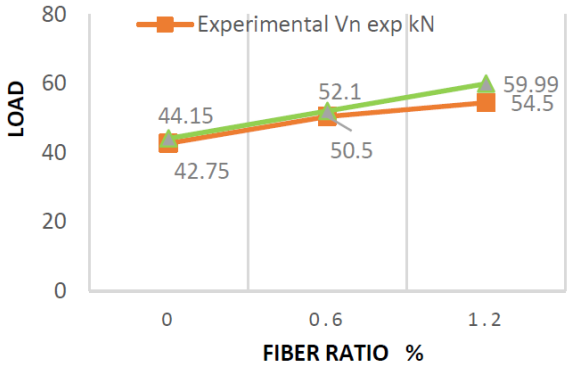

Fig. 32 Fiber ratio for the steel-reinforced GFRC beams

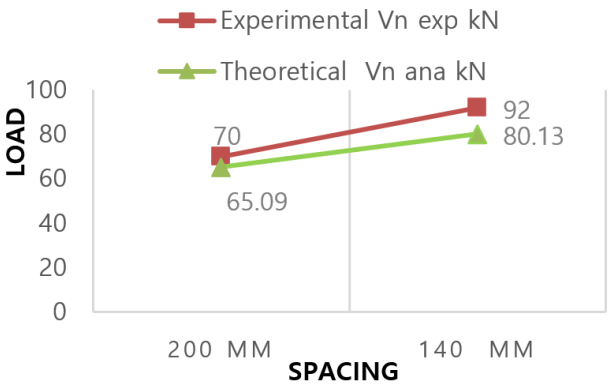

Fig. 33 NSM steel links spacing for GFRC beams

glass fiber with a rectangular section

$$D_f = \sqrt{\frac{4\ t_f w_f}{\pi}}$$

V_{gf}: volume fraction of glass fiber; d_f: bond factor: 0.5 for straight fibers with a round section, 0.75 for crimped fibers, and 1.00 for indented (hooked - end) fibers. 0.5 was used for this research for straight glass fibers with a rectangular section.; ρ: flexure reinforcement ratio.; *a/d*: shear span to depth ratio; *b*: beam web width of the cross-section (mm); *d*: is the effective depth of the beam section.

4.1.2 Contribution of GFRC by using GFRP as longitudinal reinforcement

The shear resistance of GFRC in beams reinforced with GFRP bars as flexural reinforcement and without web reinforcement ($V_{c.f}$) is calculated according to some theoretical models, the term *Af*Ef*, was compared to that of steel reinforcement, *As*Es*, to evaluate the axial stiffness of FRP longitudinal reinforcement. The following equation is recommended by ACI Committee 440 (2006) for calculating ($V_{c.f}$)

$$V_{c.f} = \frac{E_f \rho_f}{E_s \rho_s} V_C$$

Where $V_{c.f}$: Shear design strength for FRP-reinforced concrete beams; ρ_f: the reinforcement ratios of the flexural FRP reinforcement; ρ_s : the reinforcement ratios of the flexural steel reinforcement; E_f: the modulus of elasticity of FRP reinforcement; E_s: the modulus of elasticity of steel reinforcement.

These equations were also modified for beams by multiplying *Vc* by the cubic root of the ratio of the moduli of elasticity of GFRP and steel (Fariborz Farahmand 1996) as follows: *Vc x* (EGFRP/Esteel) 1/3.

When using GFRP bars instead of steel bars as tension reinforcement, the ultimate load increases slightly because of the higher tensile strength of GFRP bars, but the beam stiffness decreases (deflection increases) because of the lower modulus of elasticity of GFRP bars as compared to steel bars (Raid *et al*. 2016). Therefore, when GFRP bars are used, a balance must be struck between strength and serviceability considerations. The modified equation to calculate shear design strength for FRP-reinforced concrete beams ($V_{c.f}$) is

$$V_{c.f} = \text{Ƈø}\,(\rho_f/\rho_s)\,(E_f/E_s)^{1/3}\,V_C \qquad (3)$$

Where: as

Ƈ: the end bar Shape factor:1.2 for U shape fiber bars; ø: The Surface bar Shape factor:1.25 for serrate Surface to fiber bars.

4.2 Contribution of externally strengthened steel stirrups (links) in the carrying shear.

For the evaluation of the NSM steel link bars contribution to the shear strength, based on the experimental results, the following general equation was assumed as the shear resisted by the steel stirrups (ACI Committee 440 2008)

$$V_S = \frac{A_s f_y d}{s}(\sin\theta + \cos\theta) \qquad (4)$$

Where; A_s is the cross-section area of shear a steel link

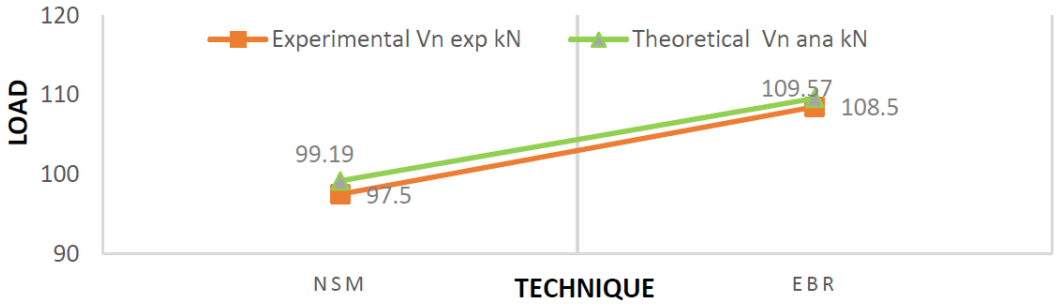

Fig. 34 NSM and EBR technique in GFRC beams

(mm^2); f_y is the tensile yield strength of shear a steel link (MPa); d is the effective depth of the beam section (mm); S is the spacing of shear a steel link reinforcement (mm); θ is the angle of shear reinforcement to the beam longitudinal axis.

4.3 Contribution of the externally strengthened FRP (links, strips, bent bars) to shear capacity of GFRC beam

According to ACI-440 (2008), the shear force resulting from the tensile stress in the FRP along the assumed crack can be calculated to determine the contribution of shear strength provided by the FRP strengthening reinforcement. The contribution of the externally strengthened FRP to shear strength is given by the following equations.

$$V_f = \frac{A_f f_{yf} d}{S_f} (\sin\theta_f + \cos\theta_f)$$

Where; V_f: the stand for the nominal shear strength provided by FRP; f_{yf} is the tensile strength for fiber; d is the depth of beam; S_f is the spacing between FRP stirrups in axis direction (mm); A_f is the area of shear fiber (mm^2); θf is the fiber inclination angle with the axis of the member.

4.3.1 Contribution of the externally strengthened FRP links. (Group 2, 3)

The contribution of GFRP links in the shear capacity of the test specimens can be analytically predicted, as follows.

$$V_{f.l} = \eta \frac{2\pi r^2 f_{yf} d}{S_f} (\text{Sin}\,\theta_f + \text{Cos}\,\theta_f) \quad (5)$$

Where: V_f: the stand for the nominal shear strength provided by GFRP links; r^2 : is the half of the diameter bar of shear fiber (mm^2); f_{yf} is the tensile strength for link fiber bar (MPa); η is the shape factor of link fiber bar: 1.0 for Straight fibers bar (Vertical and Inclined), 1.25 for Double-C-shape.

4.3.2 Contribution of the externally strengthened FRP strips. (Group 3)

The contribution of GFRC beams externally strengthened with FRP reinforcement strips to the shear capacity of beams can be calculated by the model proposed by ACI 440 as follows.

$$V_f = \frac{n W_f T_f F_f d_f}{S_f} \quad (6)$$

The proposed equation is

$$V_{f.st} = \eta \frac{2t_f w_f f_{yf} d}{S_f} (\text{Sin}\,\theta_f + \text{Cos}\,\theta_f) \quad (7)$$

Where: $V_{f.st}$: the stand for the nominal shear strength provided by FRP strips; t_f is the thickness of shear fiber strips (mm); w_f is the width of shear fiber strips (mm); d is the distance from extreme compression fiber to centroid of longitudinal tension reinforcement (mm), s_f is the center-to-center spacing between GFRP strips in axis direction (mm), η is the strengthening technique factor of fiber strips: 1.0 for NSM technique, 1.15 for EBR technique.

4.3.3 Contribution of the externally strengthened FRP bent-up bars. (Group 4)

$$V_{f.b1} = 2\pi r^2 f_{yf} (\text{Sin}\,\theta_f + \text{Cos}\,\theta_f) \quad (8).$$

$V_{f.b1}$: the stand for the nominal shear strength provided by FRP Bent up bars on one row as shown in beams B2GF-Sb1.

$$V_{f.b2} = \frac{2\pi r^2 f_{yf}\, d}{S_f} (\text{Sin}\,\theta_f + \text{Cos}\,\theta_f) \quad (9).$$

$V_{f.b2}$: the stand for the nominal shear strength provided by FRP Bent up bars on two rows as shown in beams B2GF-Sb2.

The (V_f) value may be estimated from the summation of forces in GFRP strips and bent-up bars intersecting the critical shear crack at the ultimate limit state.

Hence the GFRP strips and bent up bars contribution to shear capacity can be written as follows

$$V_f = V_{f.st} + V_{f.b1}, or V_{f.b2} \quad (10)$$

As shown in beams B2GF-Sb1- EV20F and B2GF-Sb2-EV20F.

A comparison between the experimental shear force obtained from test results $V_{n(\text{exp})}$ and analytical shear force prediction of proposed equations $V_{n(\text{ana})}$ are listed in Table 8, and the ratio $k=V_{n(\text{exp})}/V_{n(\text{ana})}$ is also indicated. Fig. 32 Shown Comparison of experimental and theoretical results of fiber ratio for the steel-reinforced GFRC beams. Fig. 33 Shown Comparison of experimental and theoretical results of NSM steel links spacing for GFRC beams. Fig. 34 Shown Comparison of experimental and theoretical results of NSM and EBR technique for GFRC beams.

It can be seen from previous results that the proposed equations have satisfactory accuracy. For steel main reinforcement, adding glass fiber by 0.6% and 1.20% decreased the shear capacity of the beam by 3% and 9%

than the predicted values of proposed equations, respectively. In the future, modified code formulas (ECP-203 and ACI 318) would be expected to account for the effect of inserting discrete glass fiber while predicting the ultimate shear strength of concrete mixed with discrete glass fiber.

5. Conclusions

An extensive laboratory testing program on the shear behavior of GFRC beams strengthened using several schemes were complete in this research, the following conclusions can be made:

- All tested beams failed in shear and strengthening techniques increased the ultimate shear strength of RC beams significantly.
- The results showed an increase in the shear stress at cracking and ultimate loads with increased fiber volume in the concrete mix.
- Test results indicated no significant influence of using GFRP longitudinal reinforcement instead of steel on the shear strength of the beams. Longitudinal GFRP reinforcement improved the shear capacity of beams without stirrups and increased ultimate shear strength by 6.4, 6.9, and 7.1% for glass fiber ratio of 0, 0.6, and1.2%, respectively, compared to beams with longitudinal steel reinforcement and a slight effect on both ductility and load-carrying capacity of the beams.
- Strengthening using inclined bars showed better performance than strengthening using vertical bars with the same spacing and provided a slight increase in the cracking and ultimate shear load by 12.5 and 12.15% respectively, for steel links and by 3.8 and 12.1%, for GFRP links.
- NSM bars twisted from strips technique provided results very close to the EBR strips technique for shear strengthening.
- It was concluded that the best strengthening technique is the combination of GFRP strips and two layers of bent bars. This led to an increase in the cracking and ultimate load by 39 and 120%, respectively compared to the control beam. Ductility was increased by 79% using this system.
- A proposed theoretical formula for shear capacity was proven to agree with the experimental data.
- The ratio between the experimental and analytical shear strength according to the proposed equation ranged from 0.91 to 0.97 for beams in groups 1 and 2. The ratios ranged between 0.99 to 1.15 in specimens with steel stirrups, 0.99 to 1.08 in specimens strengthened by links of glass fiber stirrups, 0.98 and 0.99 in specimens strengthened by closed glass fiber stirrups. In beams strengthen by bent glass fiber bars, the ratios were 0.97 to 1.07, and 0.75 to 0.82 for bent bars with stirrups.

Research recommendations

More experiments with more parameters such as concrete strength, discrete glass fiber ratio, number of GFRP layers and bent up bars, type and orientation of fiber, size of the beam, use of anchored, shear span to depth ratio, strips by NSM, strip width, strip spacing, and type of internal shear reinforcement are required for shear strengthening of GFRC beams with GFRP bars and strips.

The use of an end anchoring system at the FRP ends to configurations of FRP side-links or double-C-shape bars strengthening technique overcomes brittle de-bonding, dominating ultimate failure, and therefore allows the GFRP bars to be used to their maximum capacity. The authors will examine this as a future research topic.

In future research, we recommend by applied concrete strain in the bottom face and studying the relationship between tensile strain and compressive strain of concrete.

References

Abdul-Zaher, A.S., Abdul-Hafez, L.M., Tawfic, Y.R. and Hammed, O. (2016), "Shear behavior of fiber reinforced concrete beams", *JES. J. Eng. Sci.*, **44**(2), 132-144.

ACI 440.1R-06 (2006), Guide for the Design and Construction of Structural Concrete Reinforced with FRP Bars, Reported by ACI Committee 440, American Concrete Institute, USA.

ACI Committee 318 (2014), Building Code Requirements for Structural Concrete ACI, Vols. 318-14.

ACI Committee 440 (2008), Guide for the Design and Construction of Externally Bonded FRP Systems for Strengthening Concrete Structures (ACI 440.2R-02), American Concrete Institute, Farmington Hills, Mich.

Ahmadi, M., Kheyroddin, A., Dalvand, A. and Kioumarsi, M. (2020), "New empirical approach for determining the nominal shear capacity of steel fiber reinforced concrete beams", *Constr. Build. Mater.*, **234**(20), 117293. https://doi.org/10.1016/j.conbuildmat.2019.117293.

Al-Rousan, R.Z. and Issa, M.A. (2016), "The effect of beam depth on the shear behavior of reinforced concrete beams externally strengthened with carbon fiber–reinforced polymer composites", *Adv. Struct. Eng.*, **19**(11), 1769-1779. https://doi.org/10.1177/1369433216649386.

AlShadidi, R.M.H., Hassan, H.F. and Mohammed, M.H. (2016), "Shear behavior of high strength concrete beams reinforced with GFRP bars and strengthened by CFRP sheets", *J. Eng. Sustain. Develop. (JEASD)*, **20**(1), 102-117.

Ata, E.S.S. and Moustaf, O. (2011), "Experimental analysis of RC beam strengthened with discrete glass fiber. Facta universitatis-series", *Arch. Civil Eng.*, **9**(2), 205-215. https://doi.org/10.2298/FUACE1102205A.

Bukhari, I.A., Vollum, R.L., Ahmad, S. and Sagaseta, J. (2010), "Shear strengthening of reinforced concrete beams with CFRP", *Mag. Concrete Res.*, **62**(1), 65-77. https://doi.org/10.1680/macr.2008.62.1.65.

Chen, G.M., Teng, J.G. and Chen, J.F. (2012), "Shear strength model for FRP-strengthened RC beams with adverse FRP-steel interaction", *J. Compos. Constr.*, **17**(1), 50-66. https://doi.org/10.1061/(ASCE)CC.1943-5614.0000313.

Chen, G.M., Teng, J.G., Chen, J.F. and Rosenboom, O.A. (2010), "Interaction between steel stirrups and shear-strengthening FRP strips in RC beams", *J. Compos. Constr.*, **14**(5), 498-509. https://doi.org/10.1061/(ASCE)CC.1943-5614.0000120.

De Lorenzis, L. and Teng, J. (2007), "Near-surface mounted FRP reinforcement: An emerging technique for strengthening structures", *Compos. Part B: Eng.*, **38**(2), 119-143. https://doi.org/10.1016/j.compositesb.2006.08.003.

Dias, S.J.E. and Barros, J.A.O. (2010), "Performance of reinforced concrete T beams strengthened in shear with NSM CFRP laminates", *Eng. Struct.*, **32**(2), 373-384. https://doi.org/10.1016/j.engstruct.2009.10.001.

Dias, S.J.E. and Barros, J.A.O. (2012a), "NSM shear strengthening technique with CFRP laminates applied in high-strength concrete beams with or without pre-cracking", *Compos. Part B: Eng.*, **43**(2), 290-301. https://doi.org/10.1016/j.compositesb.2011.09.006.

Dinh, H.H., Parra-Montesinos, G.J. and Wight, J.K. (2011), "Shear strength model for steel fiber reinforced concrete beams without stirrup reinforcement", *J. Struct. Eng.*, **137**(10), 1039-1051. https://doi.org/10.1061/(ASCE)ST.1943-541X.0000362.

El-Hacha, R. and Rizkalla, S.H. (2004), "Near-surface-mounted fiber-reinforced polymer reinforcements for flexural strengthening of concrete structures", *ACI Struct. J.*, **101**(5), 717-726.

El-Sayed, A.K., El-Salakawy, E.F. and Benmokrane, B. (2006), "Shear strength of FRP-reinforced concrete beams without transverse reinforcement", *ACI Mater. J.*, **103**(2), 235.

Farahmand, F. (1996), "Shear behavior of concrete beams reinforced with glass fiber reinforced plastic", A Thesis presented to the University of Manitoba in partial fulfilment of the requirements for the degree of Master of Science

Ibrahim, A.M., Mansor, A.A. and Hameed, M. (2017), "Structural behavior of strengthened RC beams in shear using CFRP strips", *Open Civil Eng. J.*, **11**(1), 205-215. https://doi.org/10.2174/1874149501711010205.

Jin, L., Xia, H., Jiang, X.A. and Du, X. (2020), "Size effect on shear failure of CFRP-strengthened concrete beams without web reinforcement: Meso-scale simulation and formulation", *Compos. Struct.*, **236**, 111895. https://doi.org/10.1016/j.compstruct.2020.111895.

Karzad, A.S., Leblouba, M., Al Toubat, S. and Maalej, M. (2019), "Repair and strengthening of shear-deficient reinforced concrete beams using Carbon Fiber Reinforced Polymer", *Compos. Struct.*, **223**, 110963. https://doi.org/10.1016/j.compstruct.2019.110963.

Khalifa, A.M. (2016), "Flexural performance of RC beams strengthened with near surface mounted CFRP strips", *Alex. Eng. J.*, **55**(2), 1497-1505. https://doi.org/10.1016/j.aej.2016.01.033.

Medhlom, M.K. (2016), "Shear capacity of steel fiber non-metallic (GFRP) reinforced concrete beams strengthened in shear using CFRP laminates", *Civil Environ. Res.*, **8**(8), 103-117.

Monika, K., Renata, K. and Joaquim, A.O. (2017), "Influence of longitudinal GFRP reinforcement ratio on the shear capacity of concrete beams without stirrups", *Procedia Eng.*, **193**, 361-368. https://doi.org/10.1016/j.proeng.2017.06.225.

Noel, M. and Soudki, K. (2011), "Evaluation of FRP post-tensioned slab bridge strips using AASHTO-LRFD bridge design specifications", *J. Bridge Eng.*, **16**, 839-846. https://doi.org/10.1061/(ASCE)BE.1943-5592.0000226.

Panahi, M. and Izadinia, M. (2018), "A parametric study on the flexural strengthening of reinforced concrete beams with near surface mounted FRP bars", *Civil Eng. J.*, **4**(8), 1917-1929.

Said, M., Abd El-Azim, A.A., Ali, M.M., El-Ghazaly, H. and Shaaban, I. (2020), "Effect of elevated temperature on axially and eccentrically loaded columns containing Polyvinyl Alcohol (PVA) fibers", *Eng. Struct.*, **204**, 110065. https://doi.org/10.1016/j.engstruct.2019.110065.

Said, M., Adam, M.A., Mahmoud, A.A. and Shanour, A.S. (2016), "Experimental and analytical shear evaluation of concrete beams reinforced with glass fiber reinforced polymers bars", *Constr. Build. Mater.*, **102**, 574-591. https://doi.org/10.1016/j.conbuildmat.2015.10.185.

Seo, S.Y., Lee, M.S. and Feo, L. (2016), "Flexural analysis of RC beam strengthened by partially de-bonded NSM FRP strip", *Compos. Part B: Eng.*, **101**, 21-30. https://doi.org/10.1016/j.compositesb.2016.06.056.

Shanour, A.S., Said, M., Arafa, A.I. and Maher, A. (2018), "Flexural performance of concrete beams containing engineered cementitious composites", *Constr. Build. Mater.*, **180**, 23-34. https://doi.org/10.1016/j.conbuildmat.2018.05.238.

Sharaky, I.A., Torres, L. and Sallam, H. (2015), "Experimental and analytical investigation into the flexural performance of RC beams with partially and fully bonded NSM FRP bars/strips", *Compos. Struct.*, **122**, 113-126. https://doi.org/10.1016/j.compstruct.2014.11.057.

Siddika, A., Al Mamun, M.A., Alyousef, R. and Amran, Y.M. (2019), "Strengthening of reinforced concrete beams by using fiber-reinforced polymer composites: A review", *J. Build. Eng.*, **25**, 100798. https://doi.org/10.1016/j.jobe.2019.100798.

Soliman, A.E.K.S. (2012), "Efficiency of using discrete fibers on the shear behavior of RC beams", *Ain Shams Eng. J.*, **3**(3), 209-217. https://doi.org/10.1016/j.asej.2012.03.006.

Thamrin, R. and Haris, S. (2019), "Shear capacity of reinforced concrete beams strengthened with web side bonded CFRP sheets", *MATEC Web of Conferences*, **258**, 04010. https://doi.org/10.1051/matecconf/201925804010.

Zhang, S.S., Yu, T. and Chen, G M. (2017), "Reinforced concrete beams strengthened in flexure with near-surface mounted (NSM) CFRP strips: Current status and research needs", *Compos. Part B: Eng.*, **131**, 30-42. https://doi.org/10.1016/j.compositesb.2017.07.072.

PL